frontiers in Marine Science

ORIGINAL RESEARCH
published: 07 August 2019
doi: 10.3389/fmars.2019.00493

High Emissions of Carbon Dioxide and Methane From the Coastal Baltic Sea at the End of a Summer Heat Wave

Christoph Humborg[1,2], Marc. C. Geibel[1], Xiaole Sun[1], Michelle McCrackin[1], Carl-Magnus Mörth[3], Christian Stranne[3], Martin Jakobsson[3], Bo Gustafsson[1,2], Alexander Sokolov[1], Alf Norkko[1,2] and Joanna Norkko[2]*

[1] Baltic Sea Centre, Stockholm University, Stockholm, Sweden, [2] Faculty of Biological and Environmental Sciences, Tvärminne Zoological Station, University of Helsinki, Helsinki, Finland, [3] Department of Geological Sciences, Stockholm University, Stockholm, Sweden

The summer heat wave in 2018 led to the highest recorded water temperatures since 1926 – up to 21°C – in bottom coastal waters of the Baltic Sea, with implications for the respiration patterns in these shallow coastal systems. We applied cavity ring-down spectrometer measurements to continuously monitor carbon dioxide (CO_2) and methane (CH_4) surface-water concentrations, covering the coastal archipelagos of Sweden and Finland and the open and deeper parts of the Northern Baltic Proper. This allowed us to (i) follow an upwelling event near the Swedish coast leading to elevated CO_2 and moderate CH_4 outgassing, and (ii) to estimate CH_4 sources and fluxes along the coast by investigating water column inventories and air-sea fluxes during a storm and an associated downwelling event. At the end of the heat wave, before the storm event, we found elevated CO_2 (1583 μatm) and CH_4 (70 nmol/L) concentrations. During the storm, a massive CO_2 sea-air flux of up to 274 mmol m^{-2} d^{-1} was observed. While water-column CO_2 concentrations were depleted during several hours of the storm, CH_4 concentrations remained elevated. Overall, we found a positive relationship between CO_2 and CH_4 wind-driven sea-air fluxes, however, the highest CH_4 fluxes were observed at low winds whereas highest CO_2 fluxes were during peak winds, suggesting different sources and processes controlling their fluxes besides wind. We applied a box-model approach to estimate the CH_4 supply needed to sustain these elevated CH_4 concentrations and the results suggest a large source flux of CH_4 to the water column of 2.5 mmol m^{-2} d^{-1}. These results are qualitatively supported by acoustic observations of vigorous and widespread outgassing from the sediments, with flares that could be traced throughout the water column penetrating the pycnocline and reaching the sea surface. The results suggest that the heat wave triggered CO_2 and CH_4 fluxes in the coastal zones that are comparable with maximum emission rates found in other hot spots, such as boreal and arctic lakes and wetlands. Further, the results suggest that heat waves are as important for CO_2 and CH_4 sea-air fluxes as the ice break up in spring.

Keywords: heat wave, sea-air fluxes, carbon dioxide, methane, shallow coastal areas

OPEN ACCESS

Edited by:
Hans Paerl, University of North Carolina at Chapel Hill, United States

Reviewed by:
Warwick F. Vincent, Laval University, Canada
Jeffrey Chanton, Florida State University, United States

****Correspondence:***
Christoph Humborg
christoph.humborg@su.se

Specialty section:
This article was submitted to Marine Biogeochemistry, a section of the journal Frontiers in Marine Science

Received: *06 May 2019*
Accepted: *22 July 2019*
Published: *07 August 2019*

Citation:
Humborg C, Geibel MC, Sun X, McCrackin M, Mörth C-M, Stranne C, Jakobsson M, Gustafsson B, Sokolov A, Norkko A and Norkko J (2019) High Emissions of Carbon Dioxide and Methane From the Coastal Baltic Sea at the End of a Summer Heat Wave. Front. Mar. Sci. 6:493. doi: 10.3389/fmars.2019.00493

INTRODUCTION

The sheltered coastal waters and estuaries are often oversaturated with CO_2 and CH_4 as a result of high supply of autochthonous and allochthonous riverine organic matter that is partly respired in the sediments and water column (Borges and Abril, 2012). Polar amplification of global warming may lead to more frequent extreme warming events (Mann et al., 2018) in high latitude coastal systems such as the northern Baltic Sea. This, in combination with the observed redistribution of land-derived carbon from land to sea, i.e., increased riverine total organic carbon (TOC) loads (Humborg et al., 2007; Andersson et al., 2015), potentially increases respiration patterns and sea-air fluxes of CO_2 and CH_4.

The two barriers constraining CO_2 and CH_4 outgassing from marine water bodies are anaerobic and aerobic oxidation of CH_4 in the sediments and water column (Reeburgh, 2007, 2013) and limited vertical mixing across density gradients that often lead to an accumulation of CO_2 and CH_4 in deeper parts of the water column (Gentz et al., 2014). The latter barrier is particular important in the strongly stratified Baltic Sea (Jakobs et al., 2014). A portion of the CO_2 can be exported laterally with increasing salinity and pH as dissolved inorganic carbon (DIC) from the inland coastal waters to larger depths, as seen in the shallow East Siberian Sea and the central deep Arctic Ocean (Anderson et al., 2017).

Ebullition of CH_4 is often discussed as a significant source to sea-air CH_4 fluxes, but the detection and spatiotemporal analysis are poorly constrained (Leifer and Patro, 2002; McGinnis et al., 2006; Rehder et al., 2009; Weber et al., 2014; Lindgren et al., 2016). However, recent studies suggest that the deeper, vertically stratified outer parts of high latitude coastal seas, such as the East Siberian Sea or the Baltic Sea, are moderate sinks for CO_2 (Gustafsson et al., 2014, 2015; Omstedt et al., 2014; Humborg et al., 2017; Schneider et al., 2017) and that net sea-air CH_4 fluxes from the Siberian Shelf have been heavily overestimated (Parmentier et al., 2017). For example, only moderate CH_4 fluxes to the atmosphere have been reported for the open East Siberian Sea (Thornton et al., 2016) and the open Baltic Sea (Jakobs et al., 2014). In contrast, the inner parts of coastal waters and estuaries are potential hotspots of CH_4 and CO_2 outgassing (Bange et al., 1994) due to (i) the high organic matter content in coastal sediments, (ii) short residence time of gaseous compounds in the shallow water column, (iii) sediment gas release that is transported directly, as gas bubbles, to the atmosphere (meaning significantly less CH_4 oxidation within the water column), and (iv) the often high turbidity that potentially lowers primary production and CO_2 uptake.

Even if extreme weather events in coastal waters become more frequent, as predicted for the future for the Baltic Sea (Meier et al., 2012), their sampling remain difficult to schedule due to the randomness of their occurrence. However, modern instrumentation provides new opportunities; the online monitoring coastal observatory MONICOAST, near the Tvärminne Zoological Station (TZS) in southern Finland, has been recently launched to understand and visualize the impacts of long-term climate and environmental change[1]. This high-resolution monitoring station is the site of almost 100 years of weekly observations at the same station. Thus, this monitoring station constitutes one of the longest temperature records available for a coastal site in the Baltic Sea. Temperature records at 32 m water depth indicated record high temperatures of $>20°C$ at the end of the heat wave during the summer of 2018.

Previous studies have shown that the combination of high temperatures and high organic matter contents in sediments and the water column along the Belgian coast in the North Sea led to high concentrations of CO_2 and CH_4 in the water column (Borges et al., 2016). Based on these previous results and the records from TZS, revealing the exceptionally high water temperatures, we conducted our cruise at the end of the extended heat wave in the summer of 2018. The main objective of this study was to quantify emission patterns of CO_2 and CH_4 under these extreme conditions, which can be regarded as a snap-shot of future emission regimes in coastal areas. Further, we wanted to investigate whether a sharp vertical water column stratification as established mainly by a halocline in the Baltic Sea and in the East Siberian Sea but not in other areas as the North Sea act as an efficient barrier for CO_2 and especially CH_4 fluxes also in shallow coastal parts. We followed a west-east transect across the Baltic Sea starting in the Swedish Archipelago and ending in the Finnish Archipelago, crossing the deeper open parts of the Northern Baltic Proper. We investigated CO_2 and CH_4 water column inventories and sea-air exchange patterns in contrasting environments where wind mixing and upwelling/downwelling are physical drivers that may trigger outgassing events of CO_2 and CH_4. Additionally, we were able follow the break-up of the heat wave and summer stagnation that came after the first autumn storms (in this case, gale force winds) that deepened the surface water layer. By collecting continuous measurements by means of a seawater intake system, an equilibrator set-up and CO_2 and CH_4 analyzers and combing these measurements with acoustic mapping of the water column, we were able to map and follow outgassing patterns in the Finnish coastal waters over several days before, during, and after the storm. This spatially integrated and non-invasive approach allowed us to detect a high flux event across an entire bay related to extreme weather, something that needs to be considered in order to deepen our knowledge of coastal biogeochemistry and carbon processing in a warmer and potentially stormier world.

MATERIALS AND METHODS

Study Area and Cruise Track

The Baltic Sea is a semi-enclosed brackish water body consisting of a set of major relatively deep basins, shallower bays, gulfs, and archipelagoes. The most recent digital bathymetric model by the European Marine Observation and Data Network (EMODnet Bathymetry Consortium, 2018) delineates the various sub basins of the Baltic Sea that are used throughout this study and indicate the average depth of the Baltic Sea with 53 m

[1]https://www.helsinki.fi/monicoast

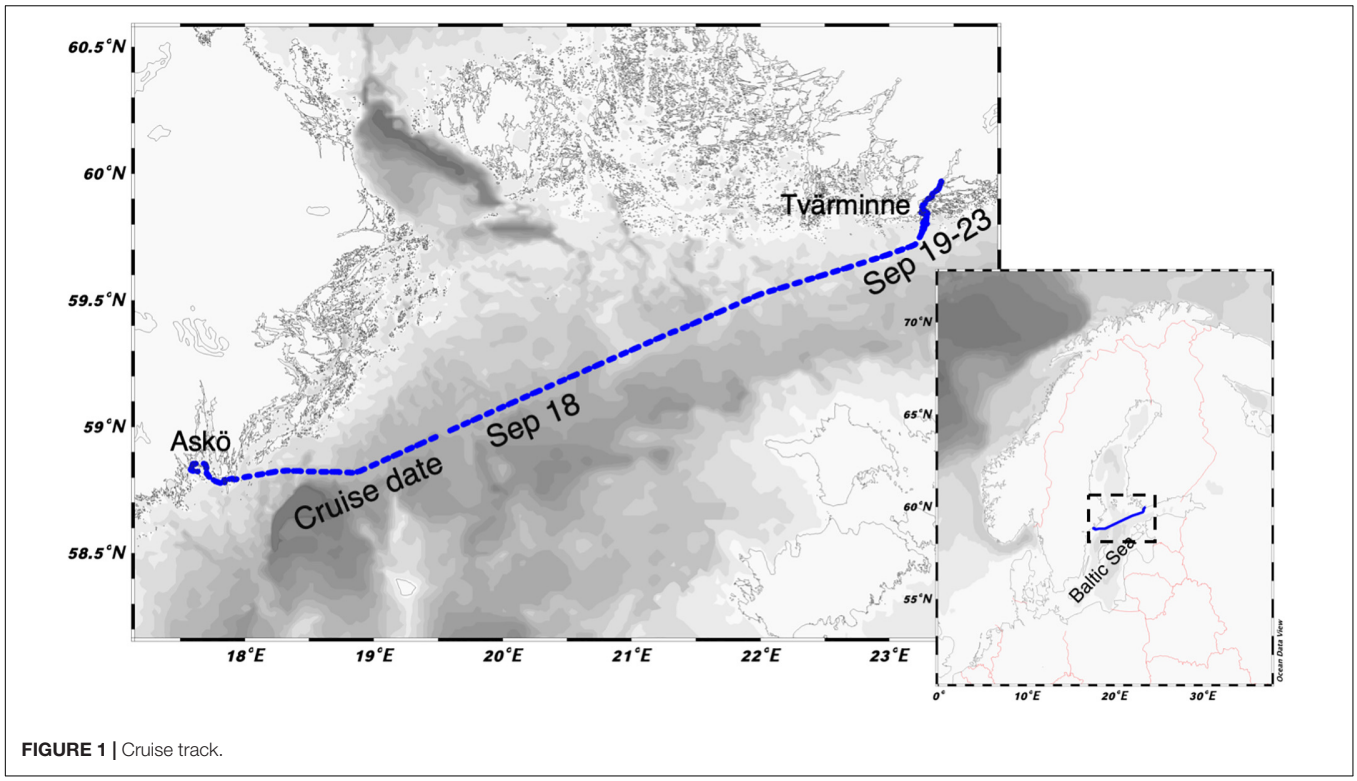

FIGURE 1 | Cruise track.

(Jakobsson et al., 2019). After the Black Sea, the central Baltic Sea is the second largest anoxic coastal water body in the world. This is due to water residence time of ∼30 years, a strong vertical salinity gradient (halocline) at 60–90 m water depth, and ongoing eutrophication (Wulff et al., 2007).

The cruise was conducted with Stockholm University's Research Vessel (RV) Electra with the aim of obtaining a comprehensive and representative picture of the distribution of CO_2 and CH_4 concentrations in surface water across the Baltic Sea, covering a broad depth range, at the end of the heat wave during the summer of 2018. We covered archipelago-type coastal seascapes of Sweden and Finland, the Northern Baltic Proper, the Åland Sea, and the Gulf Finland (**Figure 1**). In fact, these shallower coastal seascapes consisting of hundreds to thousands of semi-enclosed bays and basins make up a huge proportion of the Baltic Sea, i.e., 25% of the Northern Baltic Proper, 70% of the Åland Sea, and 60% of the Gulf of Finland are shallower than 40 m depth (Jakobsson et al., 2019). The 40 m boundary used in this study to discriminate shallower from deeper sites is chosen because it separates two concentration regimes in the Baltic Sea and the shallower parts show much more elevated concentration of CO_2 and CH_4. In general, very little is known about sea-air gas exchange in these shallow areas of the Baltic Sea, and hardly any data are available with only a few exceptions for the Gulf of Finland, i.e., the harbor areas of St. Petersburg and Helsinki (Schneider et al., 2014). For the northern boreal part of the Baltic Sea consisting of the Bothnian Bay, the Quark, the Bothnian Sea, the Gulf of Finland, and the Northern, Western and Eastern Baltic Proper the total area shallower than 40 m is some 71,000 km^2 (Jakobsson et al., 2019). For perspective, impressive data sets on water-air CO_2 and CH_4 exchange are available (Juutinen et al., 2009; Humborg et al., 2010) for Sweden and Finland, where total lake area is about 33,000 km^2 and 30,000 km^2, respectively (the Swedish lake area was estimated excepting the largest deep lakes Vättern and Vänern where no CH_4 and CO_2 exchange estimate exists).

Statistical Evaluation of Long-Term Temperature Records

The long-term temperature record from the TZS coastal monitoring site (lat: 59.85548N, lon: 23.26033E) covers August 1926 to December 2018. A moving average was adopted to smooth the short-term fluctuations in the temperature data by taking the average value of a 1-year length and shifting forward, i.e., for each average annual value calculation, the first number of the 1-year data series was excluded and the next value was included. Note that the time interval of each temperature record varied slightly, from 10 days in the years before 1997 down to 4–7 days after 1998 and finally daily records in 2018. Thus, the 1-year length used in this study is fixed from a day in a year to the same day in the year after regardless of the time interval between two specific temperature records.

Continuous CO_2 and CH_4 Measurements in Surface Water and Atmosphere

The partial pressures of atmospheric and dissolved CO_2 and CH_4 were measured using the Water Equilibration Gas Analyzer System (WEGAS) coupled to cavity ring-down spectrometer (CRDS). This system consists of three major components: (i) a

water handling system comprised of a showerhead equilibrator (1 L headspace volume) fed by the seawater intake, an E&H electrode probe and a thermosalinograph (Seabird TSG 45); (ii) a gas handling system with circulation pumps for the showerhead and ambient air from the bow of the ship; and (iii) CRDS gas analyzers for CO_2 and CH_4 concentrations (model G2131-i, Picarro Inc.); and A detailed description of the WEGAS systems and its performance can be found in the **Supplementary Material**.

Measurements of surface water CO_2 and CH_4 concentrations were performed using the seawater intake located just below the sea surface. Water was pumped through spray nozzles into the open headspace equilibrator at ∼4.5 L min^{-1}. By creating a fine spray of droplets, the exchange surface between showerhead and water was maximized and an optimal equilibration is achieved. The ambient pressure was maintained through a ambient air-fed vent flow that was monitored continuously during the measurements. The gas equilibrated in the showerhead was measured using the CRDS analyzer. For the standard CO_2 and CH_4 analysis routine, ambient air is measured for 8 min followed by the gas measurements in the showerhead of the equilibrator for 12 min, i.e., one complete analysis cycle is 20 min. Cycles are performed continuously during the cruise including the station time when RV Electra is not steaming.

Continuous CO_2 and CH_4 measurements in both ambient air and surface water were conducted during September 18–23, 2018; in total, 80,393 data points for both CO_2 and CH_4 in air and water were recorded. The recorded data were filtered by removing data taken during the transition period between ambient air and water measurements (see detailed description in **Supplementary Material**) and collected during improper functioning of WEGAS (e.g., low water flow, exceptional values due to air contamination by the ship) and thereafter the data were also corrected for the vent flow to the equilibrator that was induced while WEGAS was running. Any remaining data with CO_2 concentrations above 450 ppm were also removed. After filtering, atmospheric CO_2 averaged 401.3 ± 2.08 ppm (2σ). As a result of spatial normalization and excluding data that could have been contaminated by the ship, here we present 15,733 data points for both air and water concentrations.

For reporting the CO_2 content in water, the ppm value obtained by the cavity ring down spectrometer (CRDS) were converted to pressure units (pCO2 in μatm). We assumed ambient atmospheric pressure because water was taken at depth of around half a meter below the surface and the pressure in the showerhead is equal to ambient air as achieved by the vent flow taken at the bow of the ship.

For reporting the CH_4 concentrations in water, the ppm value obtained by CRDS were converted to molar units (i.e., nmol/L) by Henry's law (Equation 1), because the achieved equilibration means that the gas content in the showerhead is equivalent to that in the water phase, i.e., CH_4 measured by CRDS is considered as the real-time concentration of CH_4 in water. This makes Henry's law applicable for dealing with gas/liquid equilibria and the Henry's constant for molar concentration and partial pressure conversion is chosen in this case. As the showerhead in the equilibrator is maintained at ambient pressure and the water temperature is measured by thermosalinograph right before the water reaches the equilibrator, Henry's law constant is corrected for each calculation by the measured temperature at atmospheric pressure.

$$C = p \times K_{\mathrm{H}} \tag{1}$$

where C is the concentration of CH_4 (mol/L), p is the partial pressure in unit of atm (1 atm = 10^6 ppm) of CH_4. K_{H} is the Henry's law constant that is dependent on temperature and is corrected in this study following the van 't Hoff equation (Sander, 2015):

$$K_{\mathrm{H}} = K_{\mathrm{H}}^{*} \times \exp[\frac{-\Delta_{\mathrm{sol}}H}{R} \times (\frac{1}{T} - \frac{1}{T^{*}})] \tag{2}$$

Where K_{H}^{*} is the Henry's law constant at the reference temperature, 298 K, T* is the reference temperature, 298 K and T is the measured temperature in water (K). The temperature dependence of the equilibrium constant, $\frac{-\Delta_{\mathrm{sol}}H}{R}$ does not change much with temperature and is tabulated (Sander, 2015). K_{H} also varies with pressure, but in this study, pressure was assumed to be atmospheric pressure because water was taken at depth of around half a meter.

In the Baltic Sea both CO_2 and CH_4 concentrations span an order of magnitude and the highest concentrations reported are >2500 μatm of CO_2 (Fransner et al., 2019) and >1200 nM of CH_4 (Jakobs et al., 2014).

Calculations of Sea-Air Gas Fluxes

The sea-air flux (F) of CO_2 and CH_4 is commonly expressed by the following equation (Liss and Slater, 1974):

$$F = k \times (C_{\mathrm{sea}} - C_{\mathrm{air}}) \tag{3}$$

where k is the gas transfer velocity and C_{sea} and C_{air} are concentrations of gases in the sea and the overlying air, respectively. This is also frequently written as Equation 4

$$F = k \times K_0 \times \left(p_{\mathrm{sea}} - p_{\mathrm{air}}\right) \tag{4}$$

where K_0 is the solubility of CO_2 or CH_4, p_{sea} and p_{air} are the measured partial pressures of the gases in equilibrium with surface water and in the air, respectively. k is the gas transfer velocity that has been optimized as Equation 5 (Wanninkhof, 2014):

$$k = 0.251 \times U^2 \times \left(\frac{Sc}{660}\right)^{-0.5} \tag{5}$$

where U is wind speed (m/s) and Sc is the Schmidt number, which is highly dependent on temperature and gas. Sc in our calculations was corrected for the corresponding temperature that was measured simultaneously with partial pressures of CH_4 and CO_2 (pCH_4 and pCO_2).

Combining Equations 3, 4 and 5, the flux of CO_2 and CH_4 in this study is finally calculated as Equation 6:

$$F = 0.251 \times U^2 \times \left(\frac{Sc}{660}\right)^{-0.5} \times K_0 \times \left(p_{sea} - p_{air}\right) \quad (6)$$

Regional Meteorological and Oceanographic Data

Surface water temperature data observation in the open Northern Baltic Proper from the automatic buoy Huvudskär (lat: 58.9333 N, lon: 19.1667 E; 100 m water depth) were retrieved from the Swedish Hydrological and Meteorological Service[2]. Wind data observation from the Raasepori Jussarö (lat: 59.82076N, lon: 23.57309E) weather station and wave height observations from the buoy Raassepori Hästö Busö (lat: 59.82583N, lon: 23.30783E), which are located some 15 km and 5 km from the TZS, respectively, were retrieved from Finnish Meteorological Institute[3].

Box Model Approach to Address Sources and Sinks of CO_2 and CH_4

Using the surface CO_2 and CH_4 concentration in inshore and offshore surface waters and sea-air flux data and the information about the deepening of the upper mixed surface layer after the storm event, we can construct a budget evaluating the sources and sinks of CO_2 and CH_4 (**Figure 2**). The conservation of mass for the surface layer under the assumptions mentioned is:

$$h_{after} CO_{2after} - h_{before} CO_{2before} = CO_{2offshore}(h_{after} - h_{before}) - F_{CO_2}\Delta t + I_{CO_2}\Delta t \quad (7)$$

$$h_{after} CH_{4after} - h_{before} CH_{4before} = CH_{4offshore}(h_{after} - h_{before}) - F_{CH_4}\Delta t + I_{CH_4}\Delta t \quad (8)$$

Where h is the mixed layer depth before and after the storm, respectively, F atmospheric flux and I an internal source term. The source water for the advection term, i.e., $CO_{2offshore}$ *and* $CH_{4offshore}$ are assumed to have properties close to what was observed offshore on September 19 and 20.

Continuous Measurements of Gas Flares and Bubbles

The acoustic water column data presented here were continuously collected with a Simrad EK80 wideband split-beam scientific echo sounder with a center frequency at 70 kHz that was installed on RV Electra. The vertical range resolution is approximately 2 cm and the ping rate was about 2.5 Hz. The sonar produces a linear frequency modulated acoustic signal which provides improved signal-to-noise ratio and a higher vertical range resolution compared to similar narrow-band systems (Stanton and Chu, 2008). The dataset collected with the EK80 was match filtered with an ideal replica signal using a MATLAB software package version R2017a provided by the system manufacturer, Kongsberg Maritime (Lars Anderson, personal communication). Position and altitude information

[2]http://www.smhi.se/kunskapsbanken?query=huvudsk%C3%A4r+ost&doSearch=

[3]https://en.ilmatieteenlaitos.fi/download-observations

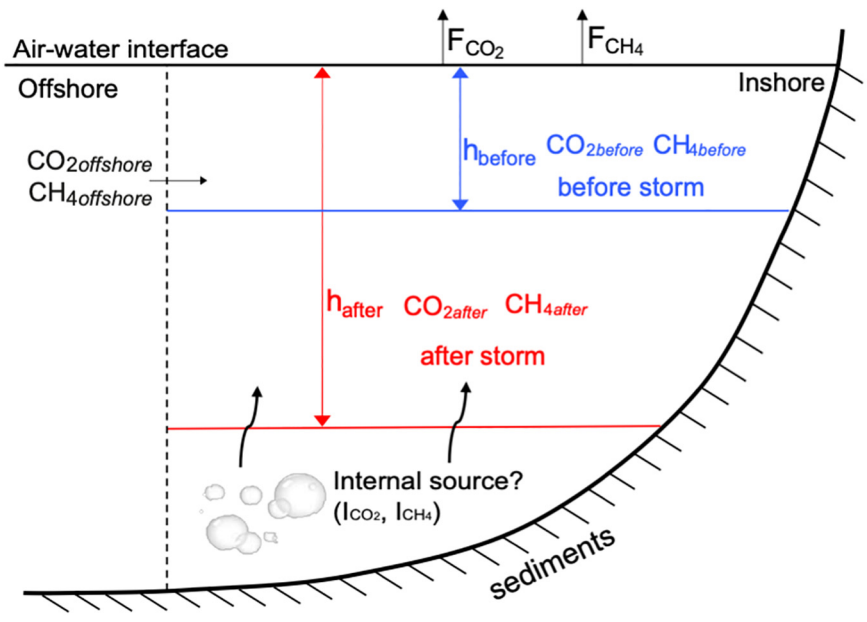

FIGURE 2 | Scheme over the budget approach evaluating the internal sources and sinks of CO_2 and CH_4 in TZS coastal waters.

were provided to the sonar by a Seapath 330 + motion sensor. Ranges from the transducer were calculated using the cumulative travel times through sound speed profile layers based on the nearest (in time) CTD profile (SEA-Bird SBE 911 plus), following the approach by Stranne et al. (2017).

RESULTS

Temperature Records in the Open Northern Baltic Proper and in the Finnish Coastal Waters Near Tvärminne

Temperatures of up to 23.04°C (daily mean) were recorded in the upper surface layer in the open Northern Baltic Proper on 6 August at the autonomous measuring stations (**Figure 3A**). A similar picture appears when evaluating the coastal monitoring stations near TZS. Since 2017, water temperatures have been continuously recorded using *in situ* instrumentation, allowing us to follow the effects of the summer 2018 heat wave in even greater detail. The highest bottom-water temperatures (32 m depth) of 20.53°C were recorded on 30 July at this coastal monitoring station (**Figure 3B**) and these are the highest temperatures ever recorded at this depth over the past 93 years. A second warming event in bottom waters above the sediments was recorded in early September 2018 just before our sampling campaign with temperatures reaching nearly 17°C (**Figure 2B**). The record-high bottom temperatures measured in the TZS area in 2018 follow an increasing trend observed over the past century until today. In **Figure 3C**, the long-term temperature record (moving average) between 1926 and 2018 is presented showing a mean water temperature of 4°C above the sediments between the 1920s and the 1980s. Thereafter, we see a dramatic increase in bottom-water temperatures starting in the 1990s to about 6°C in the 2010s.

Spatial CO_2 and CH_4 Patterns in Open vs. Coastal Areas of the Baltic Sea

Surface-water temperatures were between 14 and 18°C throughout the transect (**Figure 4A**) which is somewhat cooler than at the peak of the heat wave during July/August, when temperatures of up to 23°C were recorded in the surface layer (**Figure 3A**). Both pCO_2 and CH_4 concentrations were closer to equilibrium with the atmosphere in the central basin of the Northern Baltic Proper, but they were elevated in coastal areas (**Figures 4C,D**). However, off the Swedish coast at 70–100 m water depth, we encountered an upwelling event indicated by low temperatures and high salinity at the water surface (**Figures 4A,B**) and with elevated pCO_2 of up to >800 μatm (**Figure 4C**). CH_4 showed only moderately elevated concentrations of 12 nmol/L (**Figure 4D**). Toward the Finnish coast, both CO_2 and CH_4 gradually increased to concentrations of ∼700 μatm for CO_2 and over 30 nmol/L for CH_4. Partial pressure and concentration vs. seafloor depth plots reveal that in coastal areas, with water depths <40 m, both CO_2 and CH_4 (**Figures 5A,B**) show more elevated pCO_2 and CH_4 concentrations in the upper mixed layer compared to the open Northern Baltic Proper.

At the easternmost end of the transect, we investigated parts of Finnish Archipelago Sea near the TZS in more detail between September 19–23, 2018. pCO_2 and CH_4 concentrations followed a salinity gradient with higher values toward the freshwater end-member (**Figure 6**) that is formed by the small river Karjaanjoki (runoff 0.59 km^3 y^{-1}, Räike et al., 2012) that runs into the Pojo Bay and further into the Storfjärden Bay (black dashed box in **Figure 8A**). The highest pCO_2 (1583 μatm) was measured at the northernmost part of the Storfjärden where salinities were <5 psu. A similar pattern was recorded for CH_4, which reached its highest concentration of 70 nmol/L a bit south from the position where CO_2 peak concentrations were found. An interesting pattern appeared when plotting pCO_2 and CH_4 concentrations against seafloor depth (**Figure 7**). pCO_2 in surface water were lowest at the shallowest seafloor depth and continuously increased from 751 μatm at <5 m seafloor depth to 1020 μatm at 20–25 m seafloor depth (**Figure 7A**). In contrast, the high CH_4 concentration of 44 nmol/L (median) was recorded at the lowest seafloor depth, while concentrations ranged between 24 and 40 nmol/L at deeper depths between 5 and 25 m (**Figure 7B**). Note, that all median pCO_2 values and CH_4 concentrations were calculated before the wind event described in the next section.

Wind-Induced Changes in CO_2 and CH_4 Water Column Inventories and Inferred CO_2 and CH_4 Source and Sink Terms in Coastal Waters

Figures 8B,D show the temporal development of pCO_2 and CH_4 concentrations inshore and offshore the TZS coastal area. Elevated pCO_2 of some 800 μatm were recorded by the WEGAS system on September 19 and 20 within the inshore waters (indicated with the black dashed box in **Figure 8A**) and the offshore pCO_2 (indicated with the red dashed box in **Figure 8A**) were also at the same elevated range as the inshore concentrations (median of 740–856 μatm; **Figure 8B**). During sampling on September 21, the wind gradually increased from 5 m sec^{-1} to some 10 m sec^{-1} and pCO_2 in the inshore waters increased to 1,015 μatm, although this increase is not significant when taking the variability of the measurements in the inshore waters that day (between 700 and 1 300 μatm; **Figure 8B**) into account. Wave height increased simultaneously from 0.6 to 1.6 m. Wind speeds peaked at 20 m sec^{-1} during September 22 and decreased again down to 3 m sec^{-1} during the evening hours of September 23 (**Figure 8C**). During the same time peak wave height of 1.9 m was recorded at the monitoring buoy near TZS, which decreased to 0.5 m. Thus, during the entire period between September 19–23 the average wind was between 8 and 10 m sec^{-1} (0.5–0.8 m wave height), disrupted by the peak wind event on September 22 with wave heights of up to 1.9 m. CO_2 sea-air fluxes were greatest during this peak wind event with 274 mmol m^{-2} d^{-1} (**Figure 8C**), whereas at the end of the wind event, CO_2 was undersaturated in the upper surface layer and even negative sea-air fluxes were calculated. However, during the entire wind event, the pCO_2 decreased sharply from a 2–3 times oversaturation (median of 1015 μatm) to a slight undersaturation (median of

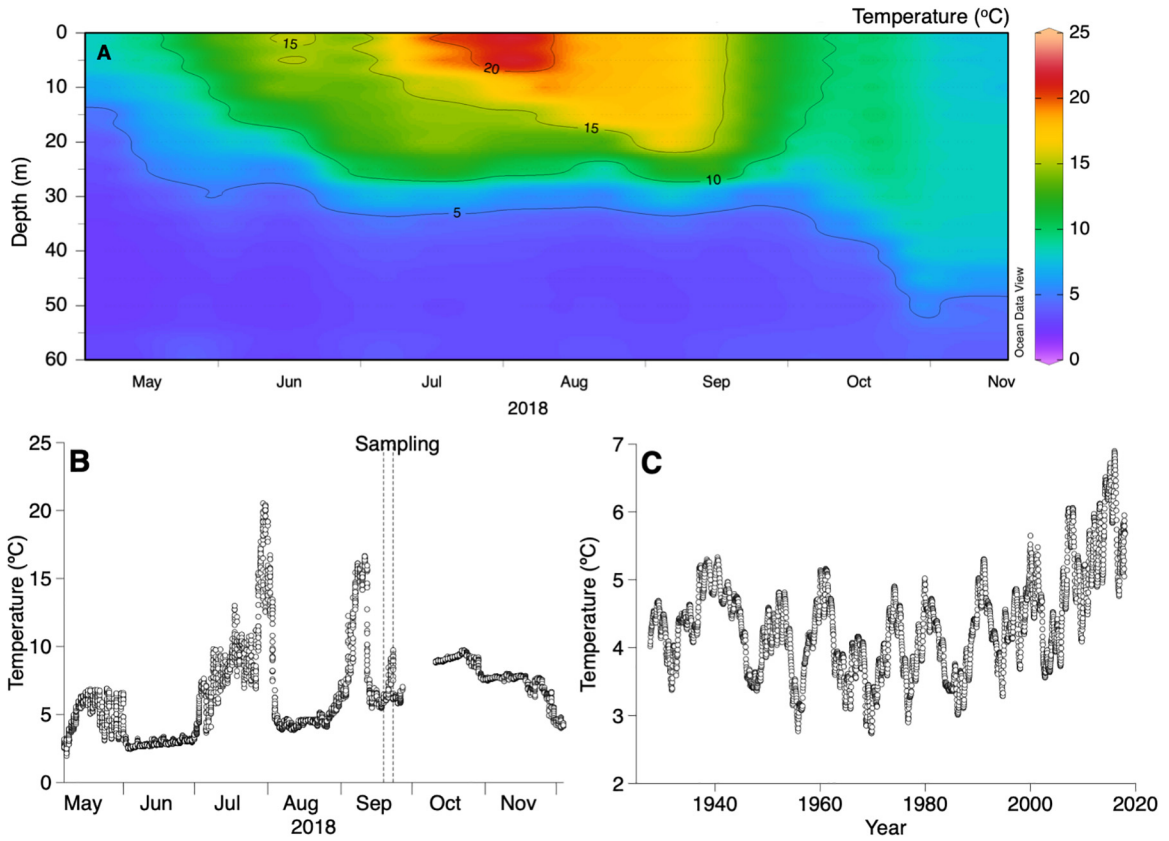

FIGURE 3 | Temperature records from **(A)** open Baltic Sea (vertical water column profile) during the heat wave in 2018 (May–November; Huvudskär, lat: 58.9333, lon: 19.1667; 100 m water depth; daily average), **(B)** bottom waters (31 m water depth) at the TZS coastal monitoring site during the heat wave in 2018 (May–November; Storfjärden, lat: 59.85548, lon: 23.26033; hourly measurements) and **(C)** bottom waters (31 m water depth) at the TZS coastal monitoring site (long-term temperature data 1926–2018; 1-year moving average).

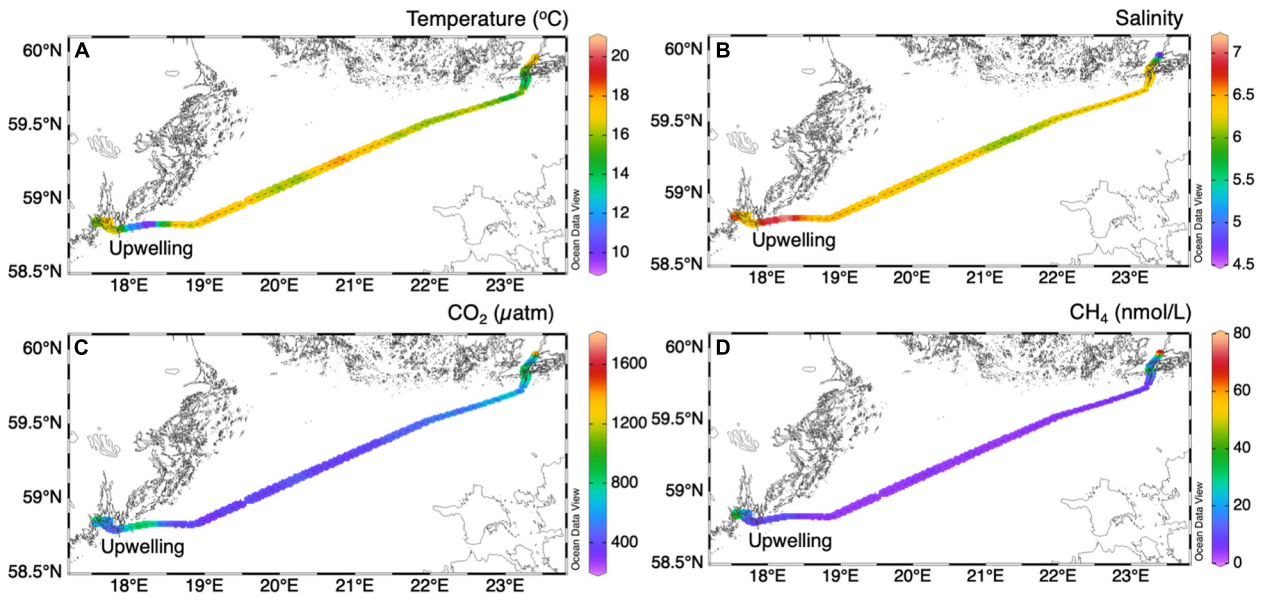

FIGURE 4 | Cross section from Askö to Tvärminne of **(A)** temperature, **(B)** salinity, **(C)** pCO_2 (µatm) and **(D)** CH_4 concentrations (nmol/L) in surface waters.

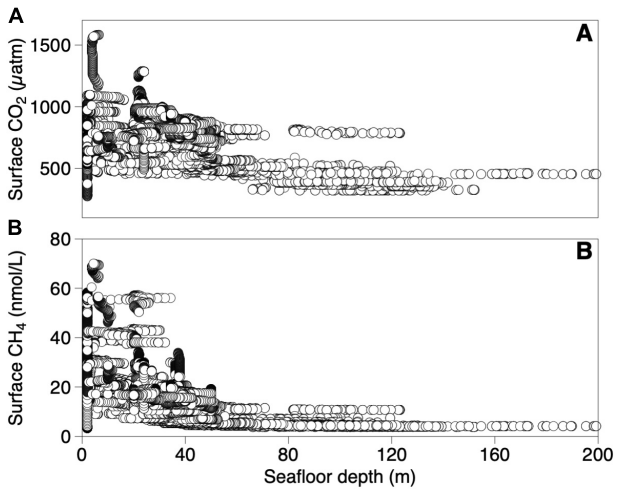

FIGURE 5 | (A) pCO_2 (µatm) and **(B)** CH_4 concentration (nmol/L) in the surface waters vs. seafloor depth along the cross section from Askö to Tvärminne.

321 µatm recorded at September 23). Thus, the wind event rather effectively depleted the water column with respect to pCO_2.

In contrast to the expected depletion of CO_2 from oversaturation caused by the wind event, CH_4 remained oversaturated before, during, and also after the wind event. Elevated CH_4 concentrations of 46 – 47 nmol/L (median; **Figure 8D**) were recorded by the WEGAS system on September 19 and 20 within the inshore waters, whereas for the offshore waters CH_4 concentrations were also supersaturated, but less so, with median concentrations between 13 and 15 nmol/L. During and after the wind event during September 22, CH_4 concentrations decreased in the inshore waters to a median value of 20–24 nmol/L, however, remained oversaturated by 5–8 times. Accordingly, the CH_4 sea-air flux calculations (**Figure 8E**) revealed the highest CH_4 average fluxes between 2.8 – 3.3 mmol m^{-2} d^{-1} before the wind event and lower, but still elevated, fluxes between 1.0 – 2.4 mmol m^{-2} d^{-1} during and after the wind event.

Although wind is directly related to the gas transfer velocity (k) in Equation 3, wind speed could only partly explain the variation in both CO_2 and CH_4 fluxes. However, the highest CH_4 fluxes were observed at relatively low winds (12 m sec^{-1}), whereas the highest CO_2 fluxes were observed at peak wind speeds (**Figures 8C,E**). Accordingly, the CO_2 and CH_4 fluxes show positive relationship (not shown), however, the highest CH_4 fluxes were recorded at very low CO_2 flux regimes, which indicates that CH_4 flux events are decoupled from CO_2 flux events during low wind regimes (9–12 m sec^{-1}).

As indicated in **Figures 8C,E**, the wind increased significantly after September 21 from less than 10 to nearly 20 m sec^{-1}. Simultaneously, CTD data collected between September 21 (10:25 UTC) and September 23 (14:00 UTC) show a deepening of the surface mixed layer after the wind event (**Figure 9**). Note that the temperature (**Figure 9B**) before and after the wind event (September 22) remained more or less constant at 11°C and that salinity (**Figure 9C**) decreased only slightly from 6.5 to 6.4 psu, whereas the upper mixed layer depth increased from roughly 10–25 m water depth. Thus, the surface mixed layer increased over these 2 days in depth from about 10 m to nearly 25 m and this was mainly caused by a downwelling event triggered by south-southeasterly winds pressing water masses into the Finnish inner coastal waters rather than by vertical mixing. Thereafter, the mixed layer depth remained at the same depth for the remainder of the cruise.

The concentrations, mixed layer depths, and atmospheric fluxes used to estimate the internal sink/source terms are given in **Table 1**. We assume that the transition occurs during 24 h corresponding to approximately the time of the storm event and the interval between the two CTD profiles mentioned above. The results of the budget calculation indicate a net sink of CO_2

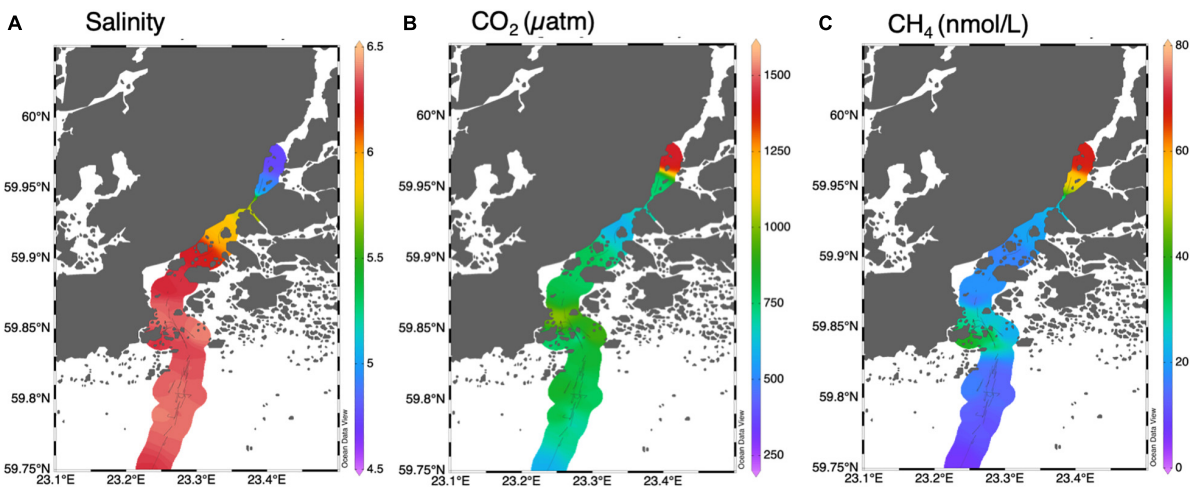

FIGURE 6 | Surface distribution of **(A)** salinity, **(B)** pCO_2 (µatm), and **(C)** CH_4 concentrations (nmol/L) within the TZS coastal waters; the black dots indicate daily cruise tracks within the area.

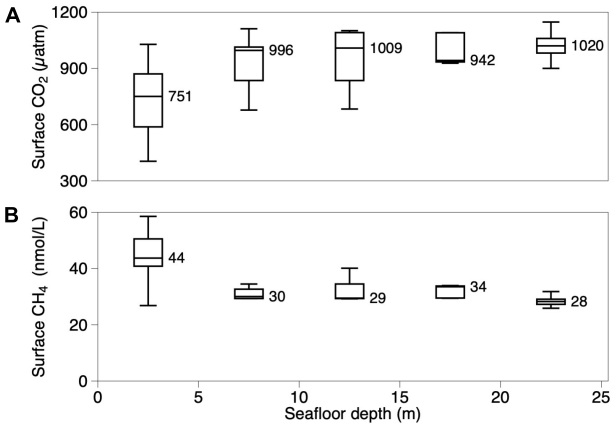

FIGURE 7 | (A) pCO_2 (µatm) and **(B)** CH_4 concentrations (nmol/L) as grouped by seafloor depth within TZS coastal waters before the storm event.

in the water column, however, the sink could be somewhat overestimated because the offshore concentrations decreased due to the massive outgassing. Further, the budget indicates a CH_4 source of about 2.5 mmol m^{-2} d^{-1} from below the mixed surface layer.

A possible explanation for the deviating patterns of CO_2 vs. CH_4 fluxes can be found in the geophysical variables investigated and continuously recorded during the cruise. The acoustic mid-water mapping revealed vigorous and widespread gas flares from the sediments in the Finnish coastal waters as exemplified in **Figure 10** where some 10–15 major flares and numerous trains of individual bubbles are visible along a 3 km transect, indicating intense bubble formation and ebullition at the sea floor. Further, gas bubbles are visible throughout the entire water column up to the water surface, penetrating into the mixed surface layer that was situated at around 10–15 m water depth (based on CTD data, **Figure 9**). The mixed layer is also discernable in the echogram, although vaguer than observations made in Arctic Ocean coastal waters (Stranne et al., 2017).

DISCUSSION

On a global scale, lakes and rivers are significant sources for CO_2 and CH_4, and their fluxes are relatively well constrained compared to the evaluation of sinks and sources in the global coastal ocean. CO_2 emissions from lakes and reservoirs are estimated to be 0.32 Pg C yr^{-1} and from rivers and streams to be 1.8 Pg C yr^{-1} (Raymond et al., 2013), whereas CH_4 emissions from inland waters are estimated to be 77 Tg C yr^{-1} (Bastviken et al., 2011). Upscaling exercises using a typology approach including four estuarine types and different types of continental shelves along three climatic zones estimates global CO_2 emissions to be 0.27 Pg C yr^{-1}, whereas global CH_4 emissions from estuaries to be 5.0 Tg C yr^{-1} (Laruelle et al., 2010; Borges and Abril, 2012). However, Laruelle et al. (2010) conclude that "the largest uncertainty of scaling approaches remains in the variability of CO_2 data to describe the spatial variability, and to capture relevant scales of variability." Note that the global estimates of coastal gas emissions are biased toward the many investigations focusing on estuaries, lagoons, salt marches, and tidal flats (Borges and Abril, 2012), whereas studies capturing shorelines that are less affected by river inputs are less studied. Further, CH_4 emissions in coastal areas are clearly coupled to temperature (Borges et al., 2016; Sawicka and Brüchert, 2017) and the highest rates of change are to be expected in organic-rich shallower parts affected by warming water bodies overlaying marine sediments. In fact, experimental studies show that a temperature increase of only 2°C can increase anaerobic organic matter degradation by 40% in marine sediments (Roussel et al., 2015). We clearly demonstrate in this study that the temperature increases in Finnish coastal waters correspond to such a 2°C rise during the last 3 decades. Bottom waters and surface sediments in this sub-arctic setting experience peak temperatures of over 20°C coinciding with elevated CO_2 and CH_4 concentrations and fluxes that are comparable to the more frequently investigated terrestrial hot spots for CO_2 and CH_4 emissions, such as arctic lakes, wetlands and thawing permafrost areas.

We suggest that the sea-air CH_4 flux is likely dominated by frequent bubbling from sediments, which we observed even during low winds, when CO_2 fluxes were at their minimum, high CH_4 fluxes occurred, knowing that this notion lacks a quantitative approach that has to be developed in the future by new ways of interpreting geophysical data of the water column. However, we have shown that surface CH_4 concentrations were highest at the shallowest seafloor depth (**Figure 7**) indicating that the proximity to the sediments and gas flares as well as the short residence times that prevent full CH_4-oxidation in the water column as observed in the deep open ocean (Reeburgh, 2007). In contrast, CO_2 in surface water shows a positive relationship with seafloor depths, indicating that respiration of autochthonous and allochthonous organic carbon in the water column is the predominant source for CO_2 even in shallow coastal systems. This has bearing for the understanding and future model parametrizations especially of CH_4 fluxes in arctic and subarctic shelf systems, i.e., a comprehensive understanding of spatial and seasonal CH_4 accumulation and flare distribution in sediments as stimulated by heat waves is needed to quantify CH_4 fluxes from shallow coastal waters. Acoustic methods directly addressing bubble-mediated methane flux are becoming more available (Weidner et al., 2019) and similar studies using mid-water sonar systems near Spitzbergen have shown that CH_4 partly originating from ebullition and transformed into the dissolved pool during upward transport is efficiently trapped below the halocline at some 200 m water depth for at least part of the year, which prevents outgassing to the atmosphere (Gentz et al., 2014). This is corroborated by our findings in the deeper stratified Northern Baltic Proper where even a strong upwelling event led to strong outgassing of CO_2 (**Figure 4C**), but only moderate increased CH_4 concentrations were observed (**Figure 4D**). Recent findings suggest that methanogenic Archaea in zooplankton guts significantly contributes to the CH_4 supersaturation in the upper surface layer of the Baltic Sea (Schmale et al., 2018), i.e., the role of bubble-mediated CH_4 transport in the central parts of Baltic appear less likely. In

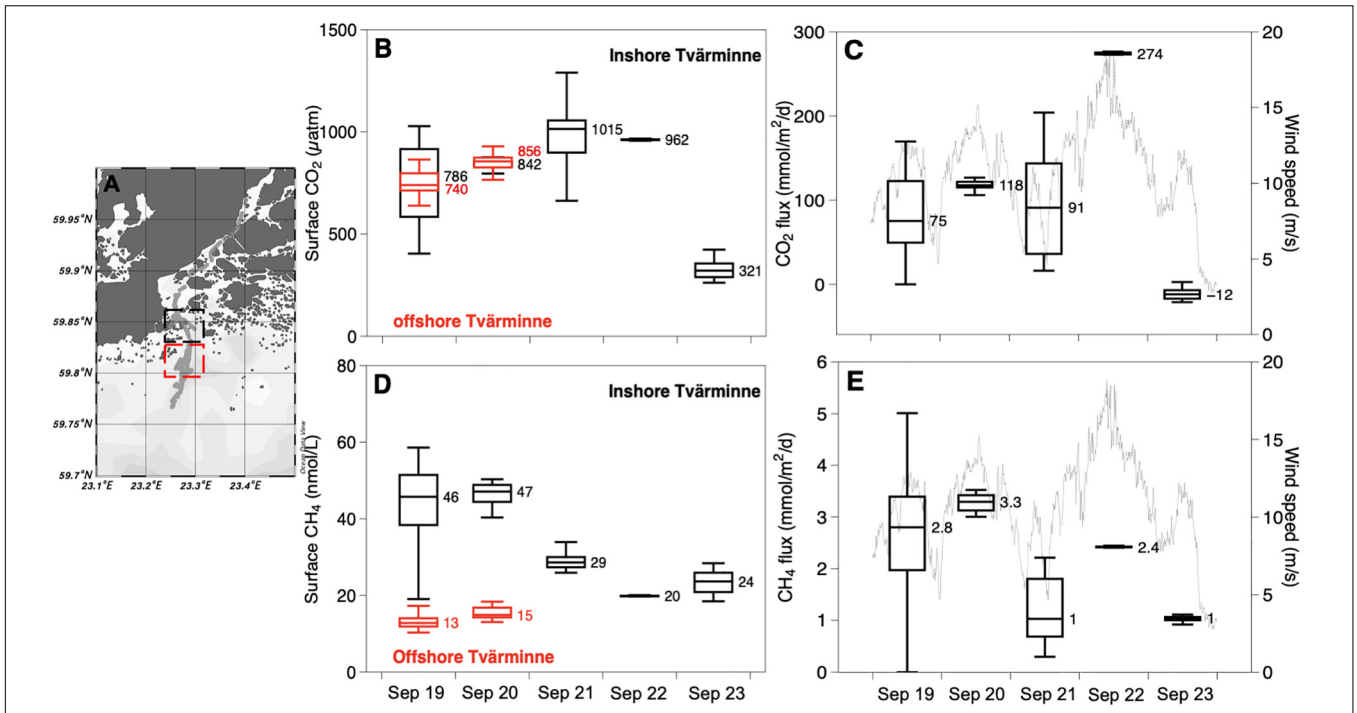

FIGURE 8 | Temporal variations in the surface waters in the inshore (black dashed square in **A**) and offshore (red dashed square in **A**) TZS coastal area **(A)** of **(B)** pCO_2 (µatm), **(C)** CO_2 flux (mmol/m^2/d), **(D)** CH_4 concentration (nmol/L) and **(E)** CH_4 flux (mmol/m^2/d) including wind speed between September 19 and 23.

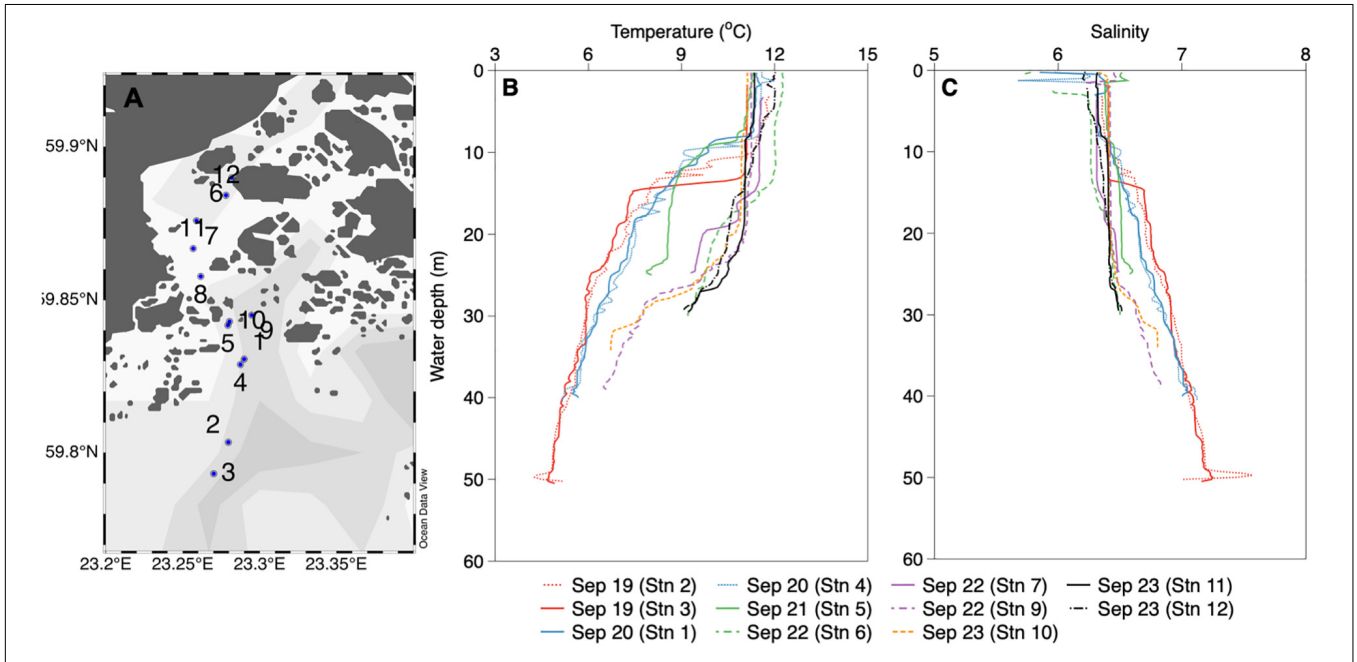

FIGURE 9 | Ventilation of the upper mixed layer in TZS coastal waters **(A)** by the storm event as demonstrated by vertical temperature **(B)** and salinity **(C)** profiles taken between 19 and 23 September 2018; position of individual CTD casts are indicated by station numbers in **(A)**.

shallow coastal areas the role of such pelagic sources may presumably be less important, because the zooplankton biomass is simply limited by the lower volume of water, but this cannot be ruled out.

We observed a pronounced pycnocline also in the coastal waters around TZS (**Figure 9**), but in this shallow coastal setting we could observe bubbles rising from the seafloor and throughout the entire water column and penetrating the

TABLE 1 | Concentrations, fluxes and mixed layer depths used in the box model calculations of CO_2 and CH_4 sources and sinks in TZS coastal waters during the storm event 21–23 September 2018.

Variables	Description	Values			
		Offshore	Before storm	After storm	During storm
CO_2	CO_2 concentration (μmol/L)	39	44	13	
CH_4	CH_4 concentration (nmol/L)	15	29	24	
h	Mixed layer depth (m)	-	10	25	
F_{CO2}	Sea-air flux of CO_2 (mmol m^{-2} d^{-1})				274
F_{CH4}	Sea-air flux of CH_4 (mmol m^{-2} d^{-1})				2.4

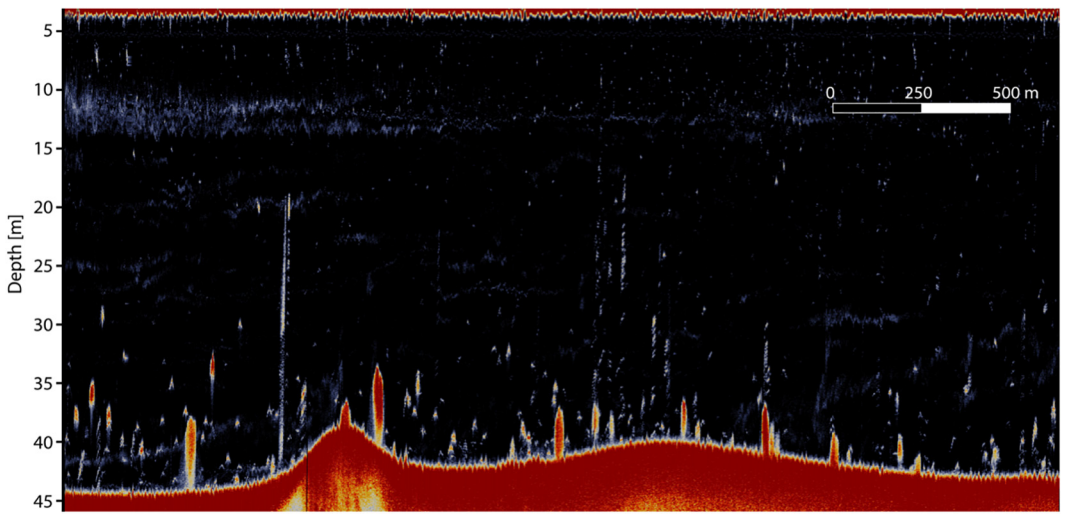

FIGURE 10 | EK80 echogram showing acoustic anomalies associated with gas seeps from the bottom sediments in TZS coastal area (black dashed square in **Figure 8A**), following the cruise track from left to right and with color indicating the acoustic target strength (black is <–80 dB and red is >–60 dB). Compass coordinates for the beginning/end of the echogram (23° 17.4′ E, 59° 49.8′ N)/(23° 16.4′ E, 59° 49.0′ N).

pycnocline (**Figure 10**). Note that the WEGAS system is capturing both diffusive and bubble flux collected by the sea water intake. We do not know whether a CH_4 reservoir has accumulated below the pycnocline in the Finnish coastal waters and thereby contributing to the elevated CH_4 concentration in the water column and significant sea-air fluxes. However, gas bubbles can only survive a certain rise height of some 100 m in the water column before they are depleted in CH_4 (McGinnis et al., 2006). Once CH_4 is dissolved, it is prone to oxidation before reaching the atmosphere and here vertical density gradients such as pycnoclines form a barrier for dissolved CH_4. This barrier to CH_4 transport from the seafloor to the atmosphere does not work in shallow coastal systems where ebullition from the seafloor can reach the atmosphere directly and our investigations show intensive bubble mediated transport between the sediments and the atmosphere down to 45 m water depth (**Figure 10**). Future investigations will show whether CH_4 concentrations in the bubbles do decrease with increasing water column travel time, i.e., whether these bubbles still contain significant amounts of CH_4 when reaching the sea-air interface. Further, it appears highly likely that the gas bubbles are of biogenic origin, because we found an inverse pattern, though not statistically significant, between CH_4 concentrations and seafloor depth and/or proximity to the shore (**Figures 6**, **7**) – a coastal effect. Eutrophication, high productivity and organic matter from runoff leads to accumulation of sediments with thick sequences of organic mud nearshore the TZS coastal area (Kauppi et al., 2018), which in turn leads to methane production and seepage. These patterns wouldn't appear when the bubbles were of thermogenic origin, i.e., from petrogenic deposits that may occur in folds that should be more randomly distributed.

A striking result of this study is that CH_4, which has a lower solubility compared to CO_2, never equilibrated with the atmosphere, whereas simultaneously the slower reacting gas (CO_2) with a higher solubility was depleted within a few hours after the wind event. Our box model approach inferred a source term for CH_4 – that might originate directly from sediment flares, or a diffusive flux from the sediments and a theoretical water column reservoir – that is significant (2.5 mmol m^{-2} d^{-1} or 30 mg C m^{-2} d^{-1}). A comparable benthic study from the nearshore shallow coastal areas along the Swedish coast (Sawicka and Brüchert,

2017) reported nearshore sediment-water fluxes between 0.1 and 2.6 mmolm^{-2}d^{-1}. Our reported rate is at the high end, indicating that the heat wave played an important role in a massive flux event of CH_4, although we have to bear in mind that the benthic sediment fluxes and fluxes from a potential reservoir in the water column cannot be disentangled from our CH_4 supply estimates. Although we do not have any quantitative measurements, the observed extensive occurrence of gas flares and bubbles point toward a significant contribution from the sediments. A comparable study addressing sea-air fluxes in the North Sea (Borges et al., 2018) report elevated fluxes between 28 and 126 mmol m^{-2} per year. Our observed accumulated flux for the 5-day period at the end of the heat wave was 11 mmol m^{-2} (averagely 2.2 mmol m^{-2} d^{-1}), which is similar to CH_4 emissions observed in thermokarst lakes in subarctic areas (Matveev et al., 2016). This result supplies further evidence that heat waves trigger massive CH_4 fluxes to the atmosphere from nearshore sites.

The sea-air CO_2 exchange of 75–274 mmol m^{-2} d^{-1} or 0.9–3.3 g C m^{-2} d^{-1} also indicates extreme outgassing during the end of the heat wave and can be compared with recent model studies indicating outgassing of up to 60 g C m^{-2} yr^{-1} in the nearshore areas of the northern Baltic Sea (Fransner et al., 2019). It is of course difficult to compare simulated annual rates with our measurements that were taken over a few days but it is, nevertheless, striking that the daily sea-air exchange rates of CO_2 presented here are one order of magnitude higher than the simulated ones. It could be that the effects of heat waves followed by increasing autumn winds for the outgassing of CO_2 haven't been considered, i.e., our 5-day estimated sea-air exchange of 6.5 g C m^{-2} is already 10% of the highest simulated annual values reproducing the spatial hot spots near the coast. The model has been calibrated/validated with ferry-box observations and clearly indicates the classical CO_2 accumulation of up to 2500 μatm under the ice and values close to equilibrium in ice-out situations. However, this study demonstrates that heat waves produce similar accumulations of CO_2 in the water column and the outgassing events can be as significant as ice-out situations that have been described also for other high latitude coastal systems, such as the East Siberia Sea (Thornton et al., 2016; Humborg et al., 2017).

CONCLUSION

In the past decade, continuously recording CO_2 and CH_4 instruments have become state-of-the-art equipment on large research vessels and on commercial ships which run ferry-box solutions. Thus, we have a fairly good understanding of CO_2 and CH_4 exchange processes in open waters of the Baltic Sea, the open Atlantic, or even in remote areas as the Siberian Sea (Körtzinger et al., 1996; Gülzow et al., 2011; Schneider et al., 2014; Thornton et al., 2016; Humborg et al., 2017). Even sediment-water exchange of CH_4 is investigated by automated lander techniques, and many of these studies focus on deeper sites (Boetius and Wenzhöfer, 2013). For the Baltic Sea and the North Sea, there are only a few datasets on nearshore shallow area emissions available and this situation may be representative for many shallow coastal systems that make up half of the Baltic Sea or a third of the global continental shelfs. In this study we show that these nearshore coastal systems are CO_2 and CH_4 emission hotspots and fluxes are comparable to terrestrial hot spot in Arctic lakes (Huttunen et al., 2006; Repo et al., 2007; Juutinen et al., 2009; Wik et al., 2013) and that shallow coastal systems are highly responsive to ongoing changes in temperature. Coastal seascapes constitute a mosaic of heterogeneous environments and habitats, and sediment-water interactions become more pertinent compared to the well-studied open coastal and ocean waters. For shallow coastal waters, the non-invasive and continuous instruments that record sediment and water column gas inventories and fluxes are still not sufficiently used and must be deployed on small research vessels that can reach the shallowest sites, which often host complex habitats such as algal belts, mussel beds, or seaweeds. The combination of the automated continuous CO_2- and CH_4-measurement devices and lander techniques, together with modern geophysics as mid-water sonar, multibeam or sub-bottom profilers, will allow identifying gas accumulations, pock marks, as well as flares and bubbles. As a result, we hypothesize that the sediment accumulation and event driven high gas emissions from nearshore shallow sediments is a major carbon capacitor in coastal areas that is not accounted for by the classical invasive core-incubation methods (Reeburgh, 1968) or by lander techniques (Boetius and Wenzhöfer, 2013) that still govern our view and process understanding of sediment-water CH_4 fluxes, and that these event-driven massive fluxes will increase with rising temperatures.

DATA AVAILABILITY

All data necessary to evaluate and build upon the work in this manuscript can be requested from the corresponding author. Atmospheric and surface water CO_2 and CH_4 data as well as CTD water profile data presented in this manuscript will be archived and freely available from the Bolin Centre Database, http://bolin.su.se/data.

AUTHOR CONTRIBUTIONS

CH wrote the manuscript and performed the measurements. MG developed the WEGAS system. XS, MM, and CM-M performed the carbon dioxide and methane measurements and did the statistical data analyses. CS and MJ did the geophysical measurements. BG did the budget calculations. AS performed the CTD measurements and analyses of wind data. AN and JN responsible for the long-term temperature measurements.

FUNDING

AN, CH, and BG acknowledge funding from the Academy of Finland (project ID 294853).

ACKNOWLEDGMENTS

This research is part of the Baltic Bridge strategic partnership between the Stockholm University and the University of Helsinki. We thank the crew and captain of RV Electra, and the staff at Stockholm Universities' field station Askö and Helsinki Universities' field station Tvärminne Zooological Station for their support. Maps were produced using Ocean Data View by R. Schlitzer, https://odv.awi.de, 2019.

SUPPLEMENTARY MATERIAL

The Supplementary Material for this article can be found online at: https://www.frontiersin.org/articles/10.3389/fmars.2019.00493/full#supplementary-material

REFERENCES

Anderson, L. G., Ek, J., Ericson, Y., Humborg, C., Semiletov, I., Sundbom, M., et al. (2017). Export of calcium carbonate corrosive waters from the East Siberian Sea. *Biogeosciences* 14, 1811–1823. doi: 10.5194/bg-14-1811-2017

Andersson, A., Meier, H. E. M., Ripszam, M., Rowe, O., Wikner, J., Haglund, P., et al. (2015). Projected future climate change and Baltic Sea ecosystem management. *Ambio* 44, 345–356. doi: 10.1007/s13280-015-0654-8

Bange, H. W., Bartell, U. H., Rapsomanikis, S., and Andreae, M. O. (1994). Methane in the Baltic and North Seas and a reassessment of the marine emissions of methane. *Glob. Biogeochem. Cycles* 8, 465–480. doi: 10.1029/94GB02181

Bastviken, D., Tranvik, L. J., Downing, J. A., Crill, P. M., and Enrich-Prast, A. (2011). Freshwater methane emissions offset the continental carbon sink. *Science* 331:50. doi: 10.1126/science.1196808

Boetius, A., and Wenzhöfer, F. (2013). Seafloor oxygen consumption fuelled by methane from cold seeps. *Nat. Geosci.* 6, 725–734. doi: 10.1038/ngeo1926

Borges, A. V., and Abril, G. (2012). "Carbon Dioxide and Methane Dynamics in Estuaries," in *Treatise on Estuarine and Coastal Science*, eds E. Wolanski, and D. S. McLusky, (Waltham, MA: Academic Press), 119–161. doi: 10.1016/b978-0-12-374711-2.00504-0

Borges, A. V., Champenois, W., Gypens, N., Delille, B., and Harlay, J. (2016). Massive marine methane emissions from near-shore shallow coastal areas. *Sci. Rep.* 6:27908. doi: 10.1038/srep27908

Borges, A. V., Speeckaert, G., Champenois, W., Scranton, M. I., and Gypens, N. (2018). Productivity and temperature as drivers of seasonal and spatial variations of dissolved methane in the southern bight of the North Sea. *Ecosystems* 21, 583–599. doi: 10.1007/s10021-017-0171-7

EMODnet Bathymetry Consortium (2018). "EMODnet digital bathymetry (DTM)," in *European Marine Observation and Data Network*, ed. E. B. Consortium. doi: 10.12770/18ff0d48-b203-4a65-94a9-5fd8b0ec35f6

Fransner, F., Fransson, A., Humborg, C., Gustafsson, E., Tedesco, L., Hordoir, R., et al. (2019). Remineralization rate of terrestrial DOC as inferred from CO2 supersaturated coastal waters. *Biogeosciences* 16, 863–879. doi: 10.5194/bg-16-863-2019

Gentz, T., Damm, E., Schneider von Deimling, J., Mau, S., McGinnis, D. F., and Schlüter, M. (2014). A water column study of methane around gas flares located at the West Spitsbergen continental margin. *Cont. Shelf Res.* 72, 107–118. doi: 10.1016/j.csr.2013.07.013

Gülzow, W., Rehder, G., Schneider, B., Schneider von Deimling, J., and Sadkowiak, B. (2011). A new method for continuous measurement of methane and carbon dioxide in surface waters using off-axis integrated cavity output spectroscopy (ICOS): an example from the Baltic Sea. *Limnol. Oceanogr. Methods* 9, 176–184. doi: 10.4319/lom.2011.9.176

Gustafsson, E., Deutsch, B., Gustafsson, B. G., Humborg, C., and Mörth, C.-M. (2014). Carbon cycling in the Baltic Sea - The fate of allochthonous organic carbon and its impact on air-sea CO2 exchange. *J. Mar. Syst.* 129, 289–302. doi: 10.1016/j.jmarsys.2013.07.005

Gustafsson, E., Omstedt, A., and Gustafsson, B. G. (2015). The air-water CO2 exchange of a coastal sea - A sensitivity study on factors that influence the absorption and outgassing of CO2 in the Baltic Sea. *J. Geophys. Res. Oceans* 120, 5342–5357. doi: 10.1002/2015JC010832

Humborg, C., Geibel, M. C., Anderson, L. G., Björk, G., Mörth, C.-M., Sundbom, M., et al. (2017). Sea-air exchange patterns along the central and outer East Siberian Arctic Shelf as inferred from continuous CO2, stable isotope, and bulk chemistry measurements. *Glob. Biogeochem. Cycles* 31, 1173–1191. doi: 10.1002/2017GB005656

Humborg, C., Mörth, C.-M., Sundbom, M., Borg, H., Blenckner, T., Giesler, R., et al. (2010). CO2 supersaturation along the aquatic conduit in Swedish watersheds as constrained by terrestrial respiration, aquatic respiration and weathering. *Glob. Change Biol.* 16, 1966–1978. doi: 10.1111/j.1365-2486.2009.02092.x

Humborg, C., Mörth, C.-M., Sundbom, M., and Wulff, F. (2007). Riverine transport of biogenic elements to the Baltic Sea - Past and possible future perspectives. *Hydrol. Earth Syst. Sci.* 11, 1593–1607. doi: 10.5194/hess-11-1593-2007

Huttunen, J. T., Väisänen, T. S., Hellsten, S. K., and Martikainen, P. J. (2006). Methane fluxes at the sediment-water interface in some boreal lakes and reservoirs. *Boreal Environ. Res.* 11, 27–34.

Jakobs, G., Holtermann, P., Berndmeyer, C., Rehder, G., Blumenberg, M., Jost, G., et al. (2014). Seasonal and spatial methane dynamics in the water column of the central Baltic Sea (Gotland Sea). *Cont. Shelf Res.* 91, 12–25. doi: 10.1016/j.csr.2014.07.005

Jakobsson, M., Stranne, C., O'Regan, M., Greenwood, S. L., Gustafsson, B., Humborg, C., et al. (2019). Bathymetric Properties of the Baltic Sea. *Ocean Sci Discuss* 2019, 1–33. doi: 10.5194/os-2019-18

Juutinen, S., Rantakari, M., Kortelainen, P., Huttunen, J. T., Larmola, T., Alm, J., et al. (2009). Methane dynamics in different boreal lake types. *Biogeosciences* 6, 209–223. doi: 10.5194/bg-6-209-2009

Kauppi, L., Norkko, A., and Norkko, J. (2018). Seasonal population dynamics of invasive polychaete genus *Marenzelleria* spp. in contrasting soft-sediment habitats. *J. Sea Res.* 131, 46–60. doi: 10.1016/j.seares.2017.10.005

Körtzinger, A., Thomas, H., Schneider, B., Gronau, N., Mintrop, L., and Duinker, J. C. (1996). At-sea intercomparison of two newly designed underway pCO2 systems - encouraging results. *Mar. Chem.* 52, 133–145. doi: 10.1016/0304-4203(95)00083-6

Laruelle, G. G., Dürr, H. H., Slomp, C. P., and Borges, A. V. (2010). Evaluation of sinks and sources of CO2 in the global coastal ocean using a spatially-explicit typology of estuaries and continental shelves. *Geophys. Res. Lett.* 37:L15607. doi: 10.1029/2010GL043691

Leifer, I., and Patro, R. K. (2002). The bubble mechanism for methane transport from the shallow sea bed to the surface: a review and sensitivity study. *Cont. Shelf Res.* 22, 2409–2428. doi: 10.1016/S0278-4343(02)00065-1

Lindgren, P. R., Grosse, G., Walter Anthony, K. M., and Meyer, F. J. (2016). Detection and spatiotemporal analysis of methane ebullition on thermokarst lake ice using high-resolution optical aerial imagery. *Biogeosciences* 13, 27–44. doi: 10.5194/bg-13-27-2016

Liss, P. S., and Slater, P. G. (1974). Flux of gases across the Air-Sea interface. *Nature* 247, 181–184. doi: 10.1038/247181a0

Mann, M. E., Rahmstorf, S., Kornhuber, K., Steinman, B. A., Miller, S. K., Petri, S., et al. (2018). Projected changes in persistent extreme summer weather events: the role of quasi-resonant amplification. *Sci. Adv.* 4:eaat3272. doi: 10.1126/sciadv.aat3272

Matveev, A., Laurion, I., Desphande, B. N., Bhiry, N., and Vincent, W. F. (2016). High methane emissions from thermocast lakes in subarctic peatlands. *Limnol. Oceanogr.* 61, 150–164. doi: 10.1002/lno.10311

McGinnis, D. F., Greinert, J., Artemov, Y., Beaubien, S. E., and Wüest, A. (2006). Fate of rising methane bubbles in stratified waters: how much methane

reaches the atmosphere? *J. Geophys. Res. Oceans* 111:C09007. doi: 10.1029/2005JC003183

Meier, H. E. M., Hordoir, R., Andersson, H. C., Dieterich, C., Eilola, K., Gustafsson, B. G., et al. (2012). Modeling the combined impact of changing climate and changing nutrient loads on the Baltic Sea environment in an ensemble of transient simulations for 1961-2099. *Clim. Dyn.* 39, 2421–2441. doi: 10.1007/s00382-012-1339-7

Omstedt, A., Humborg, C., Pempkowiak, J., Perttilä, M., Rutgersson, A., Schneider, B., et al. (2014). Biogeochemical control of the coupled CO2-O2 system of the Baltic Sea: a review of the results of Baltic-C. *Ambio* 43, 49–59. doi: 10.1007/s13280-013-0485-4

Parmentier, F.-J. W., Christensen, T. R., Rysgaard, S., Bendtsen, J., Glud, R. N., Else, B., et al. (2017). A synthesis of the arctic terrestrial and marine carbon cycles under pressure from a dwindling cryosphere. *Ambio* 46, 53–69. doi: 10.1007/s13280-016-0872-8

Räike, A., Kortelainen, P., Mattsson, T., and Thomas, D. N. (2012). 36year trends in dissolved organic carbon export from Finnish rivers to the Baltic Sea. *Sci. Total Environ.* 435–436, 188–201. doi: 10.1016/j.scitotenv.2012.06.111

Raymond, P. A., Hartmann, J., Lauerwald, R., Sobek, S., McDonald, C., Hoover, M., et al. (2013). Global carbon dioxide emissions from inland waters. *Nature* 503, 355–359. doi: 10.1038/nature12760

Reeburgh, W. S. (1968). Determination of Gases in Sediments. *Environ. Sci. Technol.* 2, 140–141. doi: 10.1021/es60014a004

Reeburgh, W. S. (2007). Oceanic methane biogeochemistry. *Chem. Rev.* 107, 486–513. doi: 10.1021/cr050362v

Reeburgh, W. S. (2013). "Global Methane Biogeochemistry," in *Treatise on Geochemistry*, 2nd Edn, eds H. D. Holland, and K. K. Turekian, (Boston, MA: Elsevier), 71–94. doi: 10.1016/b978-0-08-095975-7.00403-4

Rehder, G., Leifer, I., Brewer, P. G., Friederich, G., and Peltzer, E. T. (2009). Controls on methane bubble dissolution inside and outside the hydrate stability field from open ocean field experiments and numerical modeling. *Mar. Chem.* 114, 19–30. doi: 10.1016/j.marchem.2009.03.004

Repo, M. E., Huttunen, J. T., Naumov, A. V., Chichulin, A. V., Lapshina, E. D., Bleuten, W., et al. (2007). Release of CO2 and CH4 from small wetland lakes in western Siberia. *Tellus Ser. B Chem. Phys. Meteorol.* 59, 788–796. doi: 10.1111/j.1600-0889.2007.00301.x

Roussel, E. G., Cragg, B. A., Webster, G., Sass, H., Tang, X., Williams, A. S., et al. (2015). Complex coupled metabolic and prokaryotic community responses to increasing temperatures in anaerobic marine sediments: critical temperatures and substrate changes. *FEMS Microbiol. Ecol.* 91:fiv084. doi: 10.1093/femsec/fiv084

Sander, R. (2015). Compilation of Henry's law constants (version 4.0) for water as solvent. *Atmos. Chem. Phys.* 15, 4399–4981. doi: 10.5194/acp-15-4399-2015

Sawicka, J. E., and Brüchert, V. (2017). Annual variability and regulation of methane and sulfate fluxes in Baltic Sea estuarine sediments. *Biogeosciences* 14, 325–339. doi: 10.5194/bg-14-325-2017

Schmale, O., Wäge, J., Mohrholz, V., Wasmund, N., Gräwe, U., Rehder, G., et al. (2018). The contribution of zooplankton to methane supersaturation in the oxygenated upper waters of the central Baltic Sea. *Limnol. Oceanogr.* 63, 412–430. doi: 10.1002/lno.10640

Schneider, B., Dellwig, O., Kuliński, K., Omstedt, A., Pollehne, F., Rehder, G., et al. (2017). "Biogeochemical cycles," in *Biological Oceanography of the Baltic Sea*, eds P. Snoeijs-Leijonmalm, H. Schubert, and T. Radziejewska, (Dordrecht: Springer), 87–122.

Schneider, B., Gülzow, W., Sadkowiak, B., and Rehder, G. (2014). Detecting sinks and sources of CO2 and CH4 by ferrybox-based measurements in the Baltic Sea: three case studies. *J. Mar. Syst.* 140, 13–25. doi: 10.1016/j.jmarsys.2014.03.014

Stanton, T. K., and Chu, D. (2008). Calibration of broadband active acoustic systems using a single standard spherical target. *J. Acoust. Soc. Am.* 124, 128–136. doi: 10.1121/1.2917387

Stranne, C., Mayer, L., Weber, T. C., Ruddick, B. R., Jakobsson, M., Jerram, K., et al. (2017). Acoustic mapping of thermohaline staircases in the arctic ocean. *Sci. Rep.* 7:15192. doi: 10.1038/s41598-017-15486-3

Thornton, B. F., Geibel, M. C., Crill, P. M., Humborg, C., and Mörth, C.-M. (2016). Methane fluxes from the sea to the atmosphere across the Siberian shelf seas. *Geophys. Res. Lett.* 43, 5869–5877. doi: 10.1002/2016GL068977

Wanninkhof, R. (2014). Relationship between wind speed and gas exchange over the ocean revisited. *Limnol. Oceanogr. Methods* 12, 351–362. doi: 10.4319/lom.2014.12.351

Weber, T. C., Mayer, L., Jerram, K., Beaudoin, J., Rzhanov, Y., and Lovalvo, D. (2014). Acoustic estimates of methane gas flux from the seabed in a 6000 km 2 region in the Northern Gulf of Mexico. *Geochem. Geophys. Geosystems* 15, 1911–1925. doi: 10.1002/2014GC005271

Weidner, E., Weber, T. C., Mayer, L., Jakobsson, M., Chernykh, D., and Semiletov, I. (2019). A wideband acoustic method for direct assessment of bubble-mediated methane flux. *Cont. Shelf Res.* 173, 104–115. doi: 10.1016/j.csr.2018.12.005

Wik, M., Crill, P. M., Varner, R. K., and Bastviken, D. (2013). Multiyear measurements of ebullitive methane flux from three subarctic lakes. *J. Geophys. Res. Biogeosciences* 118, 1307–1321. doi: 10.1002/jgrg.20103

Wulff, F., Savchuk, O. P., Sokolov, A., Humborg, C., and Mörth, C.-M. (2007). Management options and effects on a marine ecosystem: assessing the future of the baltic. *Ambio* 36, 243–249. doi: 10.1579/0044-7447(2007)36%5B243:moaeoa%5D2.0.co;2

Conflict of Interest Statement: The authors declare that the research was conducted in the absence of any commercial or financial relationships that could be construed as a potential conflict of interest.